Indian Journal of Pure & Applied Physics
Vol. 56, January 2018, pp. 7-12

Studies on single step facile growth of different tin oxide nanostructures at room temperature

Sandeep A Arote[a]*& Vilas A Tabhane[b]

[a]Department of Physics, S N Arts, D J M Commerce and B N S Science College, Sangamner, Ahmednagar 422 605, India
[b]Advanced Physics Laboratory, Department of Physics, Savitribai Phule Pune University, Pune 411 007, India

Received 24 May 2017; accepted 3 November 2017

Herein, tin oxide (SnO and SnO_2) nanostructures in the form of granules, microsheets and their self-assembled flower-like morphology have been reported. The samples have been prepared by a simple single step chemical route at room temperature on a large scale. The crystalline phase, microstructural and optical properties of the nanostructures have been characterized by X-ray powder diffraction, scanning electron microscopy and UV-Vis spectroscopy. The effects of precursor concentration and reaction route on the structural, morphological and optical properties of the as synthesized sample have been investigated. The phase transition from crystalline tetragonal phases of SnO to SnO_2 has been observed as an effect of variation in NaOH concentration. The optical band gap of material has been found to be 3.05 and 3.64 eV for SnO and SnO_2, respectively. The isolated porous microspheres of SnO with diameters ranging from 12-15 μm have been observed. The growth mechanism of different morphologies has been discussed.

Keywords: Microspheres, Porosity, Optical properties, Crystal growth

1 Introduction

Preparing nanomaterials with controlled morphology, size, composition, and surface characteristics, in large scale and by simple route is a challenge in front of researcher. Consequently there is continual interest in the development of preparation techniques which are capable to synthesize the material at low cost with novel properties[1].

SnO and SnO_2 are two important wide band gap semiconductors. SnO_2 (E_g=3.6 eV) is of *n*-type semiconductor and extensively used in various applications including solar cells, gas sensors photo-catalysts and many more, due to its promising optical and electrical properties[2-5]. On the other hand SnO is also a wide band gap (2.7-3.4 eV) *p*-type semiconductor[6] which has received attention of researchers in recent years due to its applications in the various emerging fields such as sensors[7], Li-ion batteries[8], organic synthesis[9], catalyst[10], photovoltaic[11], etc. However, the preparation of SnO is relatively difficult because Sn (II) is easily oxidized to Sn (IV) in the atmosphere[12]. Numerous attempts have been made to synthesize SnO having different size and shapes viz. sheets[8], particles[13], diskettes[14], blocks[15], belts-dendrites[16], networks of ribbons[17], thin films[18], meshes[19], platelet[20], whiskers[21], bipyramids[22], flowers[23]. Various approaches like solution methods[8,23], mechano-chemistry[24], hydrothermal decomposition[21], microwave[20], ultrasound assisted solution methods[8], vapor–liquid–solid (VLS) method[16], thermal evaporation[14,15,17] and electron-beam evaporation[18] have been reported for the synthesis of same. Comparatively, three-dimensional (3D) nanostructures of SnO have been rarely studied due to its synthetic complexity and difficulty[19]. In the present work single step chemical approach is followed for the preparation of SnO and SnO_2. It avoids the use of high energetic sources for preparation of nanostructures, also no need for any vacuum. In this route, the physiochemical properties of the materials can be easily tailored just by controlling the reaction processing parameters. The prepared nanostructures are porous in nature and hence have various rooms for adsorption activity. Also the prepared nanostructures are not just the aggregation of subunits but originate from their self-assembly process. The prepared porous nanostructures may find suitable applications in the field of sensor and photocataytic degradation of hazardous compounds.

Here, we report the single step reproducible approach for synthesis of flower like porous microspheres of SnO at room temperature by wet chemical route, followed by reaction between $SnCl_2.2H_2O$ and NaOH. The effect of NaOH concentration and the reaction route, on morphology

*Corresponding author (E-mail: sandeeparote@gmail.com)

of the prepared samples and growth mechanism have been discussed in details.

2 Experimental Details

All the chemicals used in the experiment were of analytical grade and used directly without any further purification. In a typical procedure, 1 M solution of $SnCl_2.2H_2O$ was prepared using double distilled water, and then 10 mL NaOH of different concentration was added slowly to it. The whole experiment was carried out under vigorous stirring at room temperature for 15 min. The final products were cleaned several times with water and ethanol to remove the impurities and then separated by centrifugation and filtration process. Finally, the samples were dried at room temperature over the night and some amount of them annealed at 450 °C for 2 h. During synthesis it was also observed that, for 2 M NaOH the white precipitate obtained as a final product, while for 4 M NaOH, initially the solution was turbid which then turned to yellowish and finally to black precipitate.

The crystal structures of the as-prepared and annealed samples were identified by X-ray powder diffraction (XRD, Rigaku ''D/B max-2400'', X-ray diffractometer equipped with a monochromatic CuK_α radiation source λ = 1.54 Å). The morphology and content of crystallites were investigated by scanning electron microscopy (SEM, JEOL-JSM 6360-A). The UV-Vis absorption spectra were obtained by using JascoV-670 spectrometer.

3 Results and Discussion

Controlled experiments were carried out to investigate the effect of NaOH concentration and feeding method on the structural and optical properties of the as synthesized samples. However, the other reaction parameters were kept constant throughout the experiment. Figure 1 shows the XRD patterns for the synthesized samples prepared with different concentrations of NaOH. The change in phase from SnO_2 to SnO is observed by varying NaOH concentration from 2 M to 4 M and corresponds to Fig. 1(a) and 1(b), respectively. According to Fig. 1(a), XRD pattern shows diffraction from the planes of tetragonal phase of SnO_2. The diffraction data is in accordance with Joint Committee on Powder Diffraction Standards (JCPDS: 41-1445, $a = b = 4.73$, $c = 3.18$ Å). The peaks observed at different values of 2θ = 26.6°, 33.9°, 38°, 51.8°, 54.5°, 61.8° and 65.48° are assigned to diffraction from the (110), (101), (200), (211), (220), (310) and (301) planes, respectively. Remarkably it was observed that with increase in concentration of NaOH from 2 M to 4 M, the XRD data corresponds to pure tetragonal phase of SnO (JCPDS No. 06-0395, space group: P4/nmm, unit cell parameters: a=b=3.80, c=4.83 Å). The observed peaks in Fig. 1(b) at 2θ = 29.9°, 33.3°, 37.1°, 47.9°, 50.7°, 57.4°, 62.6° and 69.95°, which are assigned to the lattice planes (101), (110), (002), (200), (112), (211), (103) and (220) of tetragonal structure of SnO, respectively. The sharp and narrow diffraction peaks indicate that the material has good crystallinity.

The diffraction pattern of SnO shows larger intensity peaks with smaller full width at half maxima (FWHM) indicating highly crystalline nature compared to the SnO_2. Also no other peaks from impurities have been detected confirming the purity of synthesized samples.

Initially, the SnO_2 is formed with low concentration of NaOH (2 M), while SnO formed with increase in concentration of NaOH (about 4 M). According to

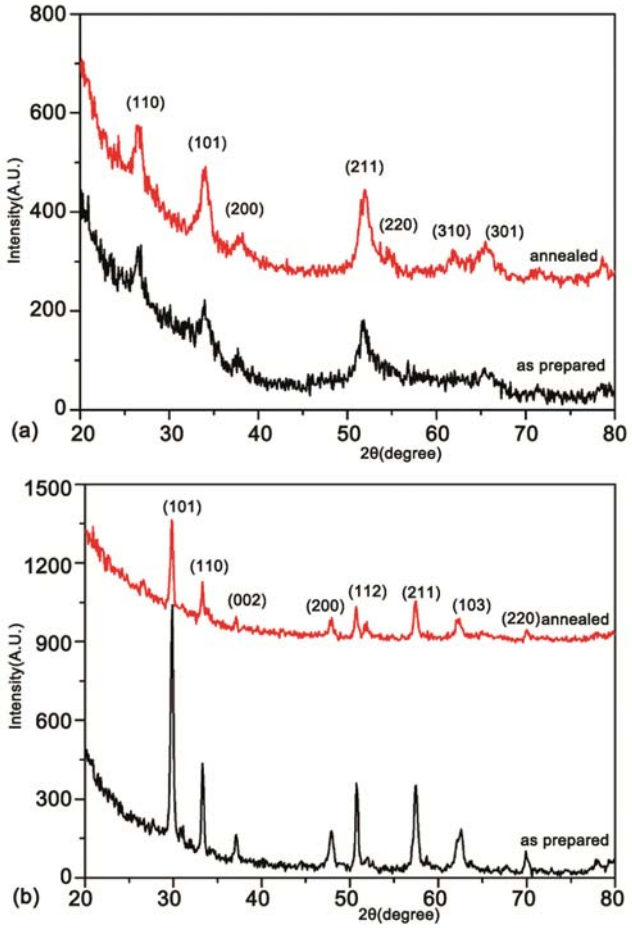

Fig. 1 — XRD pattern of as synthesized and annealed samples with NaOH of (a) 2 M and (b) 4 M concentration.

Duan *et al.*, the reverse reaction to dissociate SnO_2 to SnO could be occurred when the chemical potential change[25] $\Delta\mu$ (T, P) of the reaction ≥ 0. According to them, reverse reaction needs huge amount of energy and can only happen at very high temperature. Batzill and Diebold[26] concluded from the experimental facts that the SnO_2 was decomposed into SnO and O_2 at and above 1500 °C. Here the excess amount of NaOH even at room temperature causes change in SnO_2 to SnO. The samples are subjected to annealing to observe the change in crystallinity of the sample. No considerable change is observed in the XRD pattern for given samples even after annealing performed at 450 °C. The average crystallite sizes is calculated by using Scherrer's formula, $D = 0.89\ \lambda/\beta\ \cos\theta$, where λ is the X-ray wavelength, β is the half-width of the diffraction peak and θ is the Bragg diffraction angle[27]. Table 1 shows average crystallite size calculated for both SnO_2 and SnO. It is observed that the crystallite size for SnO is much higher than SnO_2 and is of the order of 250 nm.

The SEM images of the samples of the corresponding concentrations are shown in Fig. 2. Interestingly, the low concentration, i.e., with 2 M NaOH, aggregated nanoparticle network of SnO_2 (Fig. 2(a)) is observed and it does not show any particular morphology. While the increase in concentration up to 4 M and direct feeding of NaOH, results in formation of SnO microsheets in bundles (Fig. 2(b)) with smooth surface. Now by addition of 4 M NaOH with solvent, porous microspheres of SnO with the diameter ranging from 12 to 15 μm (Fig. 2(c)) are observed. The distribution of microspheres in the sample is random but of same fashion. From the magnified image (Fig. 2(d)), it is observed that the SnO microspheres composed with an oriented sheet-like subunit-assembled micro/nano structure with a thickness of about 120 nm and width about 500-750 nm. These microsheets are interlinked together forming an open porous structure and are expected to facilitate more interface area. The structure of the as-obtained SnO sample remains intact even after 10 min ultrasonic treatment. This specifies that the SnO microspheres are not a random aggregate but the ordered self-assembly of the microsheets. Further after annealing at 450 °C (Fig. 2(f,g), the microspheres about 8-10 μm is observed. Comparison of the images before and after annealing clearly indicates that the microspheres do not disappear but shrink in the size. The SEM results indicate that the concentration and feeding method of NaOH played an important role in controlling the morphology of the sample. The driving force for crystal nucleation and growth is supersaturation condition. At low supersaturation, crystal growth process dominates the nucleation, which results in larger clusters, while at higher supersaturation; nucleation process dominates crystal growth, resulting in smaller crystals those get oriented in a particular direction[28].

Table 1 — Average crystallite size for as prepared SnO_2 and SnO in different crystallography orientation form XRD pattern.

Sample	*hkl*	2θ (degree)	FWHM (radian)	Crystallite size (nm)
SnO_2	110	26.49	0.0051	278.33
	101	34	0.0122	117.37
	211	51.77	0.0190	80.11
SnO	101	29.86	0.00768	184.80
	110	33.3	0.00506	282.77
	002	37.09	0.00506	285.75

The optical absorption spectra for the prepared sample are obtained in the range of 200 to 800 nm to observe the effect of NaOH concentration. Figure 3(a) illustrates UV–visible absorption spectra for both samples SnO_2 and SnO. From figure, it is clearly observed that the absorbance has red shift in absorption edge due to increase in NaOH concentration. The plot of $(\text{absorbance})^2$ versus $h\nu$, (Fig. 3(b)) is used to calculate the band gap energy value for the prepared samples. The extrapolated line (the straight lines to the x-axis) shows energy band gap (E_g) about 3.05 eV for SnO and 3.64 eV for SnO_2, which is in consistent with the previous reports[6,25]. The observed E_g values are higher than that of in bulk for both the samples. The increase in energy band gap E_g is attributed to nanocrystalline nature of the sample. It is well known that the intrinsic properties of the material changes from bulk to nano by quantum size effect resulting from the decrease in the dimension of the material[29-31]. The change in E_g occurs due to transformation in density of electronic energy states as a function of quantum size effect. According to literature, some of the contribution to increase in E_g may be from porosity in the sample[32,33].

4 Growth Mechanism

Effect of NaOH concentration on obtained morphology of SnO is discussed with the help of growth mechanism. The different nanostructures grown under different synthesis routes can be explained on the basis of nucleation and crystal growth theory. Initially the number of nuclei starts

growing to cluster till certain critical size, which is thermodynamically stable. Crystal growth is preferred in a particular face which assists the system to lower its energy. Figure 4 shows the stepwise growth of SnO microspheres. The dissociation of ionic solvent in the solution, gives free anions (OH^-). The more concentration of the NaOH enhances dissociation in the solvent, which generates more ionic species[34] especially OH^-. Also, higher OH^- concentration is more preferable for growth and formation of 1D nanostructure[35] with of SnO. It means that, as reaction time prolongs, more and more nanoparticles forms network to lower their surface energy and appears nearly like sheet due to the hydrophobic interactions and Vander Waals

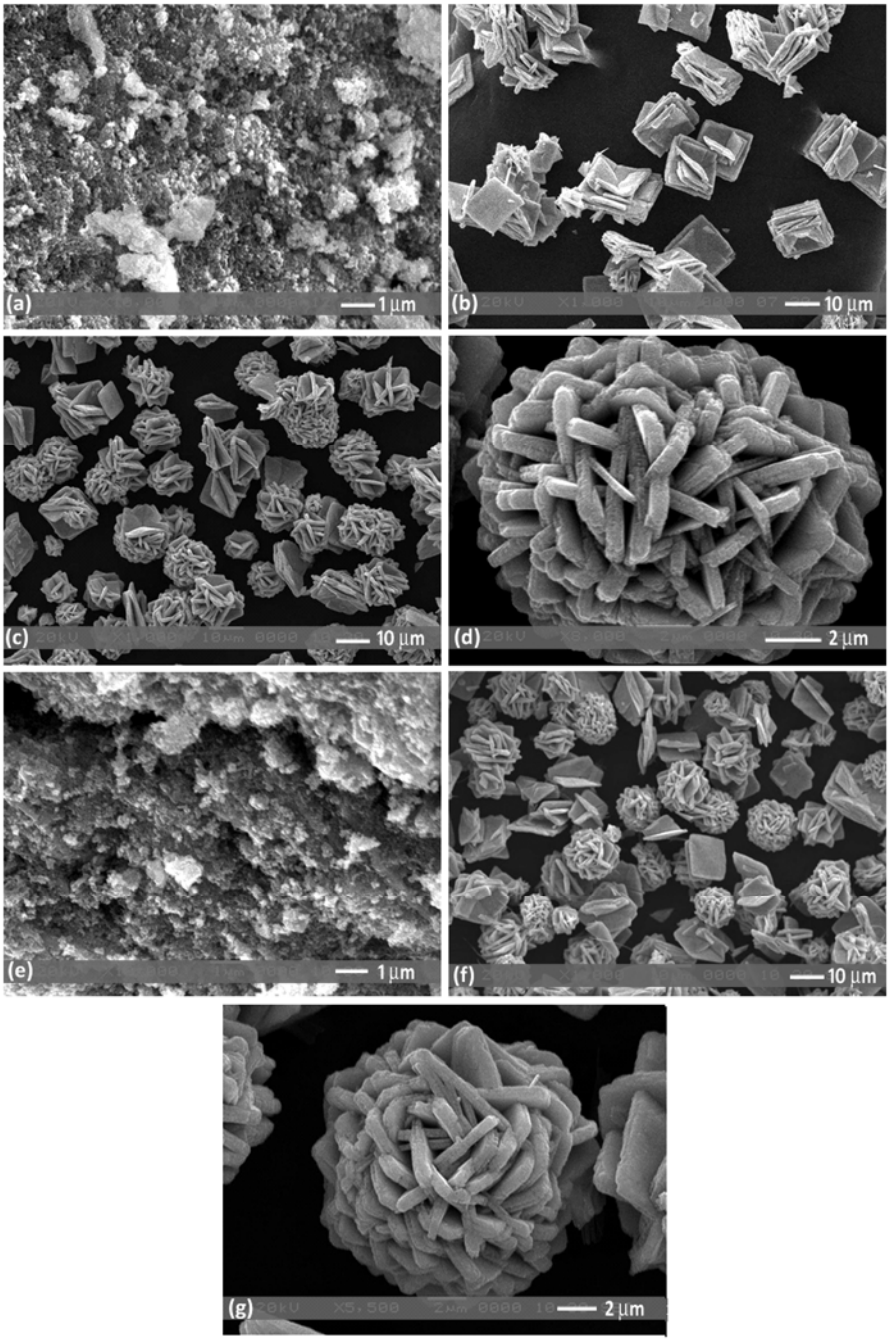

Fig. 2 — Morphology of the as-synthesized SnO nanostructures at different NaOH concentrations. SEM images of as-prepared sample with NaOH of (a) 2 M, (b) direct addition of 4 M, (c, d) addition of 4 M via solvent; SEM images of annealed sample of (e) 2 M and (f, g) 4 M NaOH.

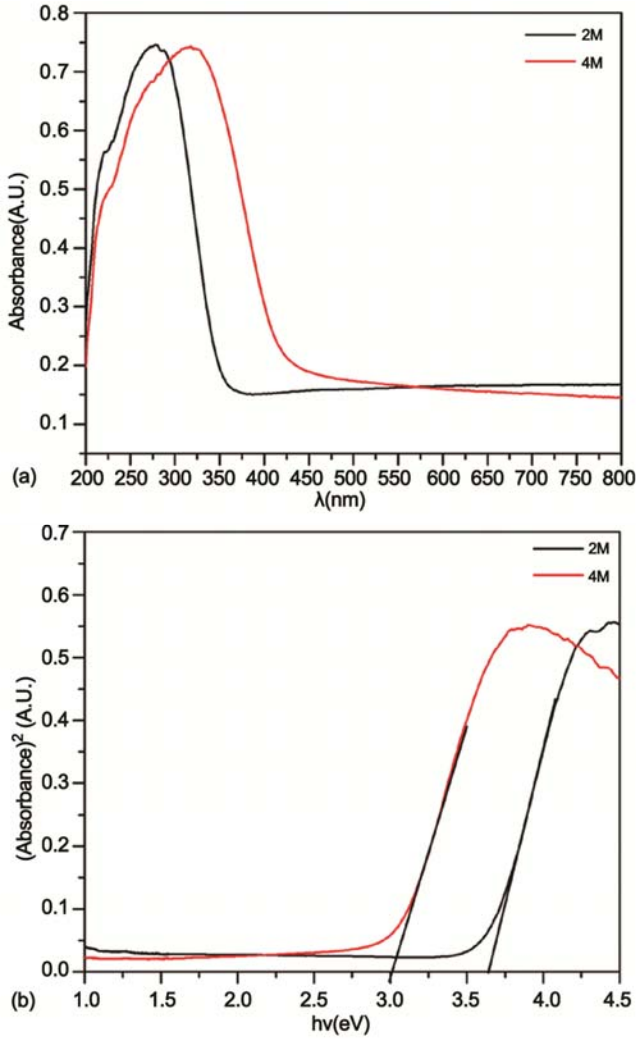

Fig. 3 — (a) Absorption spectra and (b) optical band gap calculation of samples with NaOH of 2 M and 4 M concentrations.

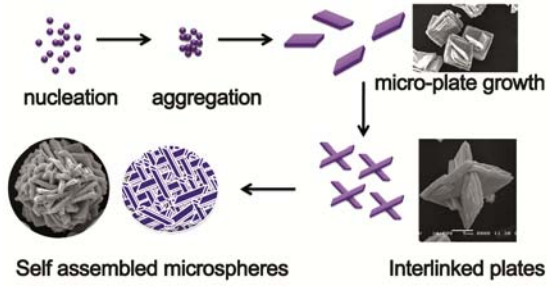

Fig. 4 — Schematic illustration of growth process of SnO microspheres.

attraction[36]. The formed microsheets then interlinked together in oriented fashion to give sphere like porous morphology. It is also well reported that, the (110) plane has higher energy than other, therefore the growth along the <001> direction can release more energy[35-37] (Gibbs-Thomson law). Thus, aggregation of nanoparticles or microsheets along particular direction causes the decrease in system energy[37]. Therefore, simply by adjusting the OH^- concentration in the solvent, these sheets aggregated to form distinct hierarchical SnO microspheres.

5 Conclusions

In summary, a very simple and low-cost chemical route has been reported for the preparation of tin oxide crystals with different morphology and phases at room temperature. The phase of tin oxide transformed from SnO_2 to SnO with change in morphology from nanoparticle-network to microsheets and further to porous microspheres observed with increasing concentration and controlled feeding rate of NaOH. The synthesized microspheres are present in pure tetragonal phase of SnO and are composed of several pieces of microsheets with thickness of about 120 nm. The interconnected microsheets within the microsphere provide the pores which will be beneficial for several applications including photocatalyst, sensor, photovoltaics and Li-ion batteries. The finding may shade some light on obtaining of controlled morphology and shapes of other materials also.

Acknowledgement

The authors are grateful to all the members of Advanced Physics Laboratories for their help in conducting the experiments. SAA is thankful to Principal, Sangamner College, Sangamner, for encouragement and constant support.

References

1 Whitesides G M & Grzybowski B, *Science*, 295 (2002) 2418.
2 Q Wang H, D Wang W & Wang T M, *Nano-Micro Lett*, 3 (2011) 34.
3 Raghupathi P S, George J & Menon C S, *Indian J Pure Appl Phys*, 43 (2005) 620.
4 Roy A, Arbuj S, Waghadkar Y, Shinde M, Umarji G, Rane S, Patil K, Gosavi S & Chauhan R, *J Solid State Electrochem*, 21(1) (2017) 9.
5 Khan I, Yamani Z & Qurashi A, *Ultra Sonochem*, 34 (2017) 484.
6 Su Z, Zhang Y, Han B, Liu B, Lu M, Peng Z, Li G & Jiang T, *Mater Des*, 121 (2017) 280.
7 Idota Y, Kubota T, Matsufuji A, Maekawa Y & Miyasaka T, *Science*, 276 (1997)1395.
8 Pei Y, Wang S, Zhou Q, Xie S H, Qiao M H, Jiang Z Y & Fan K N, *Chin J Chem*, 25 (2007) 1385.
9 Banerjee M & Roy S, *Org Lett*, 6 (2004) 2137.
10 Banerjee M & Roy S, *Chem Commun*, 534 (2003).
11 Wang Z J, S Qu C, Zeng X B, Liu J P, Tan F R, Bi Y & Wang Z G, *Acta Mater*, 58 (2010) 4950.
12 Giefers H, Porsch F & Wortmann G, *Solid State Ionics*, 176 (2005) 199.
13 Aurbach D, Nimberger A, Markovsky B, Levi E, Sominski E & Gedanken A, *Chem Mater*, 14 (2002) 4155.

14 Dai Z R, Pan Z W & Wang Z L, *J Am Chem Soc*, 124 (2002) 8673.
15 Dai Z R, Pan Z W & Wang Z L, *Adv Funct Mater*, 13 (2003) 9.
16 Orlandi M O, Leite E R, Aguiar R, Bettini J & Longo E, *J Phys Chem B*, 110 (2006) 6621.
17 Wang Z L & Pan Z W, *Adv Mater*, 14 (2002) 1029.
18 Pan X Q & Fu L, *J Electroceram*, 7 (2001) 35.
19 Ning J, Dai Q, Jiang T, Men K, Liu D, Xiao N, Li C, Li D, Liu B, Zou B, Zou G & Yu W W, *Langmuir*, 25 (2009) 1818.
20 Krishnakumar T, Pinna N, Kumari K P, Perumal K & Jayaprakash R, *Mater Lett*, 62 (2008) 3437.
21 Jia Z J, Zhu L P, Liao G H, Yu Y & Tang Y W, *Solid State Commun*, 132 (2004) 79.
22 Uchiyama H & Imai H, *Langmuir*, 24 (2008) 9038.
23 Uchiyama H, Ohgi H & Imai H, *Cryst Growth Des*, 6 (2006) 2186.
24 Kozma G, Kukovecz A & Konya Z, *J Mol Struct*, 834 (2007) 430.
25 Duan Y, *Phys Rev B*, 77 (2008) 045332.
26 Batzill M & Diebold U, *Prog Surf Sci*, 79 (2005) 47.
27 Abbas S S & Aboud H, *J Electron Mater*, 46 (2017) 1.
28 Takiyama H, *Adv Powder Technol*, 23 (2012) 273.
29 Chand P, Gaur A, Kumar A & Gaur U K, *Mater Sci Semicond Proc*, 38 (2015) 72.
30 Sonia S, Jayram N D, Kumar P S, Mangalaraj D, Ponpandian N & Viswanathan C, *Superlattices Microstruct*, 66 (2014) 1.
31 V Koutu, Shastri L & Malik M M, *Mater Sci Poland*, 34 (2016) 819.
32 Zhang H, Wu R, Xu H, Li F, Wang S, Wang J & Zhang T, *RSC Adv*, 7 (2017) 12446.
33 Kosinova A, Wang D, Baradács E, Parditka B, Kups T, Klinger L, Erdélyi Z, Schaaf P & Rabkin E, *Acta Mater*, 127 (2017) 108.
34 Zhou X F, Hu Z L, Fan Y Q, Chen S, Ding W P & Xu N P, *J Phys Chem*, 112 (2008) 11722.
35 Penn R L & Banfield J F, *Science*, 281 (1998) 969.
36 Hou B, Xu Y, Wu D & Sun Y, *J Mater Sci*, 42 (2007) 1397.
37 Ning J, Jiang T, Men K, Dai Q, Li D, Wei Y, Liu B, Chen G, Zou B & Zou G, *J Phys Chem*, 113 (2009) 14140.